PFG 2013 / 3, 0209–0220
Stuttgart, June 2013

Article

Unsupervised Change Detection on SAR images using a New Fractal-Based Measure

Hossein Aghababaee, Jalal Amini, Teheran, Iran, Maio-Li Yu-Chang Tzeng, Maio-Li, Taiwan & Josaphat Tetuko Sri Sumantyo, Chiba, Japan

Keywords: change detection, fractal geometry, wavelet multi-resolution, SAR image

Summary: Change detection for land use/cover is very important in the application of remote sensing. This paper proposes a new fractal measure for automatic change detection in synthetic aperture radar (SAR) images. The proposed measure is computed based on the fractal dimension and intensity information. The fractal dimension is calculated using the wavelet multi-resolution analysis based on the concept of fractional Brownian motion. In the next stage, a binary decision is made at each pixel location to determine whether it is a change or not, by applying a threshold on the image derived from the proposed measure. The threshold is computed from the distribution of the proposed fractal measure using the well-known Otsu method. The proposed change indicator is compared to the classical log-ratio detector as well as two other statistical similarity measures, namely Gaussian Kullback-Leibler and cumulant-based Kullback-Leibler detectors. Experiments on simulated and real data show that the proposed approach achieves better results than the other detectors.

Zusammenfassung: *Unüberwachte Detektion von Veränderungen in SAR-Bildern mit einem neuen Fraktal-basierten Veränderungsmaß.* Die Detektion von Veränderungen der Landnutzung bzw. der Bodenbedeckung ist eine wichtige Anwendung der Fernerkundung. In diesem Beitrag wird ein neues Maß für die automatische Erkennung von Änderungen in Radarbildern mit synthetischer Apertur (SAR) auf Basis von Fraktalen vorgeschlagen. Dieses Maß wird aus der fraktalen Dimension und der Intensität der SAR-Bilder bestimmt. Die fraktale Dimension wird auf Basis einer Analyse mit mehrskaligen Wavelets berechnet und beruht auf dem Konzept der fraktalen Brownschen Bewegung. Anschließend wird in jedem Pixel eine binäre Entscheidung dahingehend getroffen, ob eine Veränderung vorliegt oder nicht, indem ein Schwellwert auf das Veränderungsmaß angewandt wird. Dieser Schwellwert wird aus der Verteilung des Veränderungsmaßes mit Hilfe der Otsu-Methode abgeleitet. Der vorgeschlagene Veränderungsindikator wird mit dem klassischen log-Verhältnis-Detektor sowie mit zwei anderen statistisch motivierten Ähnlichkeitsmaßen verglichen, nämlich mit dem Gaußschen Kullback-Leibler- und dem kumulierenden Kullback-Leibler-Detektor. Untersuchungen mit simulierten und realen Daten zeigen, dass der vorgestellte Ansatz bessere Ergebnisse liefert als andere verwendete Detektoren.

1 Introduction

Detection of the changes occurring on the Earth's surface by means of multi-temporal remote sensing images is one of the most important applications of remote sensing technology. It depends on the fact that, for many public and private institutions, the knowledge of the dynamics of either natural resources or man-made structures is a valuable source of information in order to make decisions. Satellite and airborne remote sensing sensors have proven to be particularly useful in addressing change detection applications related to environmental monitoring, agricultural surveys, urban studies, and forest monitoring (Bazi et al. 2005). In remote sensing earth monitoring, unlike optical sensors, SAR sensors can

www.schweizerbart.de
DOI: 10.1127/1432-8364/2013/0171 1432-8364/13/0171 $ 3.00

acquire data day and night regardless of the cloud cover. Furthermore, in comparison with the optical sensors, data obtained by SAR sensors show great potentials for monitoring applications in some cloudy regions. Moreover, SAR images contain additional information like image coherence by acquiring interferometric images while considering critical baseline length, which could be a nice feature for change detection. In remote sensing applications, change detection is the process of identifying the differences in the state of a land cover or land use by analyzing a pair of images acquired in the same geographical areas at different times (Singh 1989).

Change detection between two optical images can easily be addressed by using difference-based indices. However, this task is much more difficult when it comes to SAR images due to the speckle effect. It is worth mentioning that speckle can be modelled in spatial chaotic systems and characterized by its fractal dimension (Tzeng et al. 2007). In the case of SAR acquisitions, the standard detector is based on the ratio of images. Bujor et al. (2004) did a very interesting job by analyzing the higher order statistics for change detection in SAR images. They concluded that the ratio was useful for step changes and that the second and third order log-cumulants were beneficial for progressive changes appearing in consecutive images of multi-temporal series. Inglada & Mercier (2007) presented a similarity measure for automatic change detection in multi-temporal SAR images. This measure was based on the evolution of the local statistics for the images between two epochs. The local statistics were estimated using a cumulant-based series expansion which approximates the possible density functions in the vicinity of each pixel in the image. The evolution degree of the local statistics was measured using the Kullback-Leibler divergence. When only a Gamma distributed texture is considered, the first moment gave the complete evolution of the texture (Mercier et al. 2008). Unfortunately, texture in medium resolution SAR images does not always follow a Gamma distribution. Hence, using an improper model might result in poor performance. For interesting approaches related to the change measures in SAR images, the reader can refer to the works of Erten et al. (2012), Bovolo & Bruzzone (2008) and Shiyong et al. (2011).

The main problems of change detection in SAR images are as follows: 1) generating a change measure or a change indicator, 2) suppression of the speckle effect and 3) thresholding the change measure to produce a binary change map. The overall performance of the detection system will depend on both the quality of the change measure and the quality of thresholding plus the speckle effect. In order to deal with the speckle and the change measure problem, a new fractal measure is proposed. It combines the fractal dimension, which is computed by the wavelet multi-resolution analysis based on the concept of the fractional Brownian motion, with the intensity information provided by the original SAR images. Finally using a threshold, a binary decision is automatically taken at each pixel location to determine whether there is a change or not. This threshold is determined from the distribution of the fractal measures employing the well-known Otsu method (Otsu 1979). The main contribution of this paper is to propose a new fractal measure which utilizes both the original SAR image information and fractal dimensions simultaneously in an unsupervised change detection process.

Fractal geometry is able to describe complex forms and find out their underlying order. The concept of fractals was introduced by Mandelbrot (1982). It can be defined as an entity for which the Hausdorff-Besicovitch dimension exceeds the topological dimension. Simply speaking, the fractal dimension of a phenomenon is a measure of randomness or variability. This dimension is different from the traditional dimensions of Euclidian geometry. Another characteristic of fractals is self-similarity, which means that fractal dimension will be the same regardless of the measurement scale. Since 1989, fractals have been extensively adopted in satellite image processing (Cola 1989, Ramstien & Raffy 1989), and fractal models have been used in a variety of image processing and pattern recognition applications. For example, several researchers have applied fractal techniques to describe image textures, data fusion, and classification (De Jong & Burrough 1995, Myint 2003, Sun et al. 2005).

The rest of the paper is organized as follows: Section 2 introduces the proposed fractal measure and the Otsu method, section 3 presents the experimental results of applying the fractal measure to both simulated and real data, and section 4 concludes the paper, proposing some directions for future works.

2 Proposed Fractal Measure

As mentioned above, the main problems of change detection in SAR images are generating a change measure or some change indicators and thresholding the change measure so that a binary change map is produced. A new fractal measure is proposed to address the former and the speckle effect while the well-known Otsu method is adopted to deal with the latter. It is known that many natural surfaces show fractal behaviour within a certain range of scales. Such behaviour is summarized by the concept of fractal dimension, which can be related to the intuitive concept of surface roughness (Pentland 1984). Fractional Brownian motion (fBm) is the most suitable mathematical model for the random fractal found in nature. Specifically, a fBm surface function $V_H(x,y)$ is described by a random field having zero-mean Gaussian increments and satisfying the relation (Betti et al. 1997):

$$E\left[\left|V_H(x,y) - V_H(x+\Delta x, y+\Delta y)\right|\right] = \\ = \left\|(\Delta x, \Delta y)\right\|^H \quad (1)$$

In (1), $E[.]$ is the expected value, $\|.\|$ is the Euclidean norm, and H is he Hurst index, or persistence factor, controlling the roughness of the surface, with $0 < H < 1$. $H = 1$ corresponds to a smooth surface and $H = 0$, to a very rough texture; for $H = 0.5$ the ordinary Brownian motion is obtained. The fractal dimension D and the Hurst index H are related by (2.1), in which E is the Euclidean dimension. The Euclidean dimension for an image is 2 ($E = 2$), so the (2.1) can be written in the form of (2.2) (Peitgen & Saupe 1987):

$$D = E + 1 - H \quad (2.1)$$

$$D = 3 - H \quad (2.2)$$

Many researchers have already shown that the SAR signal is chaotic and follows fBm (Mcdonald et al. 2002, Goodman 1976). According to Tzeng et al. (2007), the SAR signals can be modelled by a nonlinear dynamic system and are characterized by their fractal dimension.

To find the changes between two SAR images that have been registered to each other, a new fractal change measure M_{fractal} is calculated from the normalized log-ratio of the intensities of two SAR images and the normalized difference of two fractal images (3).

$$M_{fractal} = \sqrt{\left|D_{I2} - D_{I1}\right|^2 + \left|\log\left(\frac{I_2}{I_1}\right)\right|^2} \quad (3)$$

In (3), $|.|$ is the absolute value, I_2 and I_1 are the original SAR intensity images at two distinct times, and D_{I2} and D_{I1} are the corresponding fractal images. In addition to the intensity information, the proposed fractal measure considers the self-similarity character of SAR images via the fractal images. The fractal images provide information about the texture of the image, which means that the fractal measure is sensitive to texture changes.

To compute a fractal image for each pixel of the original SAR image, the fractal dimension D is estimated using the information inside a local window. Thus, the fractal dimension of each pixel depends on its neighbourhood. In this paper, a window of 7×7 pixels is used to measure D locally. Calculating the fractal dimension (or H) of remotely-sensed images with different methods gives different dimension values, because remotely-sensed images are not strictly self-similar and may, instead, be at most only statistically self-similar over a limited range of pixel sizes (Sun et al. 2006).

It has been shown that the wavelet analysis technique gives very accurate estimations of H in comparison to other classical methods (Stewart et al. 1993). The present method is derived from the peculiar form of the power spectrum of fBm. Since fBm is not a stationary process, fractional Brownian motion does not have a power spectrum defined in its classical sense. Nevertheless, fBm, being an isotropic random field, can be characterized by a random phase Fourier description that follows

a generalized power density of the form (Parra et al. 2003):

$$S(w_1, w_2) = \left| FFT(Window) \right|^2 . \quad (4)$$

In (4), w_1 and w_2 are the two axes in the frequency domain, S is the power spectrum and FFT is the fast Fourier transformation of the selected window. By filtering the frequency domain signal (S) with a wavelet filter, the resulting spectrum at a specific resolution j is (Mallat 1989):

$$S_{2^j}(w_1, w_2) = S(w_1, w_2) \left| \Psi_{2^j}{}^3(2^{-j}(w_1, w_2)) \right|^2 . \quad (5)$$

In (5), $\psi_{2j}{}^3(w_1,w_2) = \psi_{2j}(w_1)\ \psi_{2j}(w_2)$ corresponds to the 2-D wavelet associated to the diagonal details filter, and $\psi_{2j}(w_1)$ and $\psi_{2j}(w_2)$ are the one dimensional wavelet functions associated with the scaling functions $\phi(w_1)$ and $\phi(w_2)$ respectively (Mallat 1989). The subscript 2^j represents the specific resolution at which the wavelet filter is applied to the signal. The energy of the detailed signal (σ_{2j}) at a specific resolution j can be calculated by its summation in the support of $\psi_{2j}{}^3(w_1, w_2)$ of the chosen wavelet filter:

$$\sigma_{2^j}^2 = \frac{2^{-2j}}{4\pi^2} \sum_{-2^j\pi}^{2^j\pi} \sum_{-2^j\pi}^{2^j\pi} S_{2^j}(w_1, w_2) dw_1 dw_2 \quad (6)$$

The ratio of the energies corresponding to the detail signals at successive resolutions provides a solution for the computation of H as:

$$H = \frac{1}{2} \log_2 \left(\sigma_{2^j}^2 / \sigma_{2^{j+1}}^2 \right) . \quad (7)$$

In this work, H is computed using the energy of the detailed signal at the first two resolution levels ($j = 1$ and $j = 2$). After computing the Hurst index H according to (7), the local fractal dimension can be obtained by (2).

To sum up, the procedure for computing the fractal image is as follows.

In each location of the moving window:

1. Compute the power spectral density of the window according to (4).
2. Filter the computed power spectrum with a wavelet filter at two successive resolutions.
3. Measure the energy of the detailed signal at each resolution by summing up all of its elements (6).
4. Calculate fractal dimension related to the window using (7) and (2).

After computing the measure $M_{fractal}$ using (3), a binary decision is automatically made at each pixel location using a threshold derived from the histogram of $M_{fractal}$ using Otsu's method. Considering the fact that the change measure is presented by the intensity function $f(x,y)$ and the values of the measure are normalized between 0–255, the pixels on the measure can be divided into two classes $C_1 = \{0,1,\ldots,T\}$ and $C_2 = \{T+1, T+2,\ldots,255\}$ where the classes correspond to the foreground (objects of interest) and the background, respectively, and T is the desired decision threshold. The probabilities of the two classes are:

$$w_b(T) = \sum_{i=0}^{T-1} p(i), \quad w_f(T) = \sum_{i=T}^{255} p(i), \quad p(i) = \frac{n_i}{n} \quad (8)$$

In (8), w_b and w_f are the probabilities of background and foreground clusters, respectively, n_i is the number of pixels with the intensity i and n is total number of pixels in the given change measure image. Using discriminating analysis, Otsu (1979) showed that the optimal threshold T can be determined by minimizing the within-class variance (σ^2_{within}). This parameter is difficult to minimize, but it has been shown that the minimization of within-class variances is tantamount to the maximization of between-class variance ($\sigma^2_{between}$).

$$\sigma^2_{between}(T) = \sigma^2 - \sigma^2_{within}(T) = w_b(T)\ w_f(T)[\mu_b(T) - \mu_f(T)] \quad (9)$$

In (9), σ^2 is the variance of all image elements, which is constant (and not related to T), and μ_b and μ_f are the mean intensity values of background and foreground clusters, respectively. One should select the threshold T so that the between-class variance is maximized. Evaluating (9) for all possible values of T, the value that maximizes $\sigma^2_{between}$ is chosen as the final threshold.

3 Experimental Results

The proposed measure was compared to the classical log-ratio detector in order to evaluate its performance. Two other change measures, namely Gaussian Kullback-Leibler detector (Gaussian KLD) and cumulant-based Kullback-Leibler detector (cumulant-based KLD), introduced in (Inglada & Mercier 2007), are also compared. It should be noted that both Gaussian and cumulant-based KLD are computed using a 7 × 7 moving window. Experiments were carried out on both simulated and real data.

3.1 *Experiments with Artificial Change Image*

Simulations were performed to understand the behaviour of the detectors for a given type of change in a better way. As shown in Fig. 1(a), a HH polarized TerraSAR-X scene of Barcelona (Spain) (size: 400 × 400 pixels), taken on May 15, 2011 with 3 m spatial resolution was used. The images are publicly available at Astrium (2012). Three areas were changed by pasting values copied from some other area into the original image. This type of change can occur when there is a land-use change, anthropogenic activities, etc. (Inglada & Mercier 2007). The simulated change image is shown in Fig. 1(b). Changes in urban, agriculture, and water areas were simulated in the regions highlighted in Fig. 1(c). The change indicator or change measure can also be useful by itself. Indeed, the end-user of a change map often does not only want the binary information (changed vs. unchanged) but also an indicator for the intensity of change and eventually a confidence level. In this paper, the so-called receiver operating characteristics (ROC) curve is used to evaluate the quality of a change measure. The ROC plot shows the detection probability P_{det} as a function of the false alarm probability P_{fa} using different values of the threshold value T. The area under the ROC curve (AUC) is frequently used as a summary measure. The perfect ROC curve has an AUC of 1.

To evaluate the performance of change measures, different levels of speckle noise were artificially added to the SAR images to imitate the natural speckle in SAR images. The speckle noise was added using the multiplicative noise equation $J = I + \xi \cdot I$, where ξ is uniformly distributed random noise with mean 0 and variance v and J and I are the noisy and original images, respectively. In this work, the proposed fractal measure, log-ratio detector, Gaussian and cumulant-based KLD are computed from the TerraSAR-X images with noise added to them at three different levels corresponding to three values of v (0.01, 0.03, 0.05). Then the corresponding ROC curves are plotted in Fig. 2.

According to Figs. 2(a) to 2(c), the proposed fractal measure presents the best performance and the pixel-wise log-ratio detector shows the worst performance in all cases because, unlike

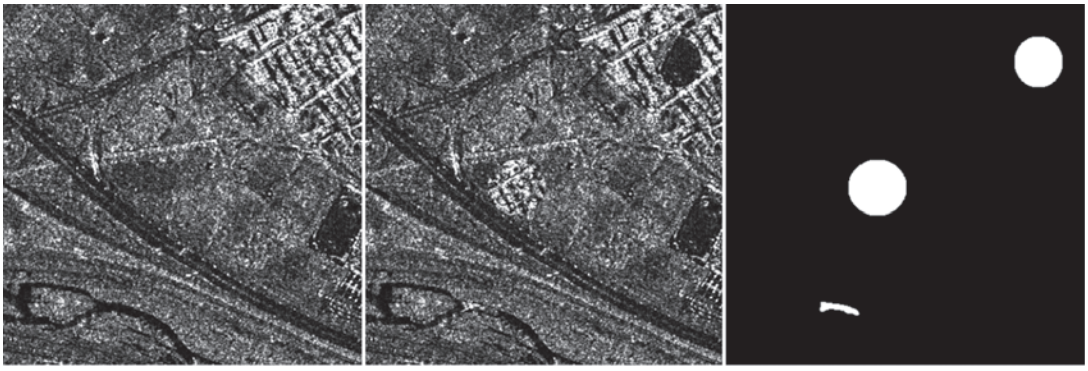

(a) Original SAR image (b) Artificial change image (c) Mask

Fig. 1: Simulation of changes on TerraSAR-X image.

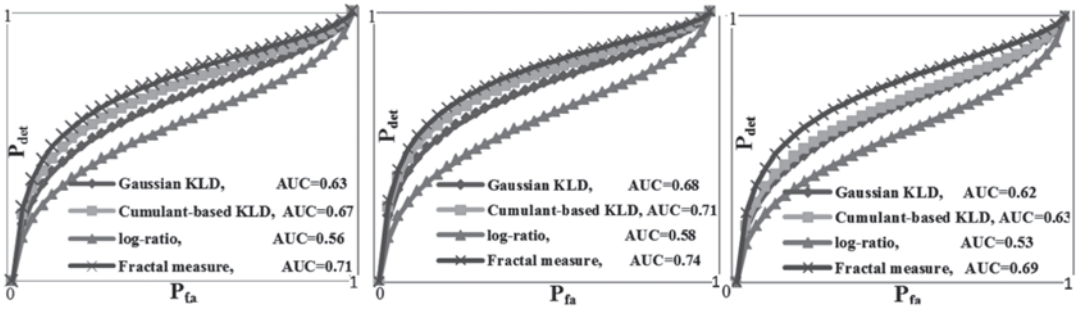

Fig. 2: ROC plot comparison of the four detectors for a simulated change in different speckle noise levels (ROC = receiver operating characteristics).

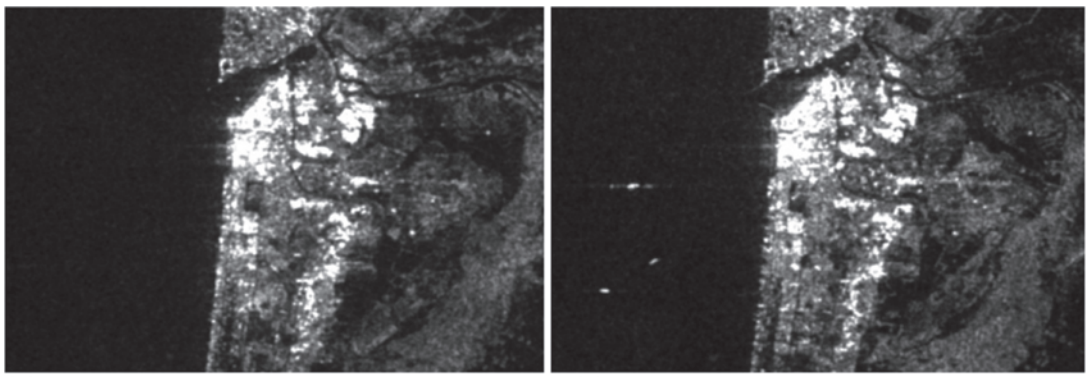

Fig. 3: Original JERS-1 images related to the first study area (Bandar-e-Anzali).

the other measures, the log-ratio image does not involve a window operation. The performance of each detector in different noise levels is quantitatively compared in Fig. 2 using AUC. Considering Fig. 2, it is clear that the fractal measure outperforms the others in different noise levels. Compared to other change detectors, the proposed fractal measure results in an improvement of up to 10 % in AUC (0.63 vs. 0.69 in Fig. 2(c)).

3.2 *Experiments with Real Data*

Two examples of applying the proposed method to real cases are presented in this subsection. The first study area is located in the north of Iran near the city of Bandar-e-Anzali. A pair of HH polarized JERS-1 images acquired in November 18, 1992 and April 4, 1997 with 18 m spatial resolution is shown in Figs. 3(a) and 3(b), respectively. The size of the images is 700 × 480 pixels. The proposed fractal measure, log-ratio detector, Gaussian and cumulant-based KLD are computed from the real dataset and a visual comparison of all measures is shown in Fig. 4. No speckle reduction was carried out, so that the resulting change measures are still affected by speckle. The quantitative comparison is made using the red and blue pixels, which are marked on the images showing the change measures (Fig. 4). The red and blue pixels represent the reference for change and unchanged regions, respectively. The reference regions for the change pixels (768 pixels) were selected in pier and residential areas, which were constructed in Anzali between 1992 and 1997, whereas the unchanged pixels (964 pixels in total) were obtained by manually analyzing the SAR images.

After determining the change measures, we derived a threshold according to the Otsu method for each measure (section 2), and we apply the thresholds to generate binary images showing at each pixel whether there is a

change according to the respective measure or not. Subsequently, all the resultant binary images are refined using a median filter with the size of 3 × 3 to remove single change pixels. The smoothed binary images are change maps in which changed and unchanged pixels are represented in white and black, respectively (Fig. 5). To compare the change detection performance quantitatively, user's and producer's as well as the overall accuracy of the change map are presented in Tab. 1.

As it can be seen in Figs. 4(a) and 5(a), the quality of the log-ratio detector is very poor and its result is unacceptable because it is seriously affected by the speckle. On the other hand, as demonstrated in Figs. 4(d), 5(d) and Tab. 1, the quality of the proposed fractal measure is more satisfactory than the other implemented methods. Apparently, speckle is modelled properly by the proposed fractal measure, and as a result its effect on the results is reduced. The change measure and change

Tab. 1: Quantitative comparison of the change maps in the first real dataset (Bandar-e-Anzali) (KLD = Kullback-Leibler Divergence).

	Unchanged		**Change**		
Overall Accuracy (%)	User's Accuracy (%)	Producer's Accuracy (%)	User's Accuracy (%)	Producer's Accuracy (%)	**Method**
73.2	93.0	56.1	63.2	94.7	**Log-Ratio**
83.3	82.1	89.6	85.3	75.4	**Gaussian KLD**
79.5	78.4	87.1	81.2	69.9	**Cumulant KLD**
89.7	85.7	97.8	96.7	79.4	**Fractal measure**

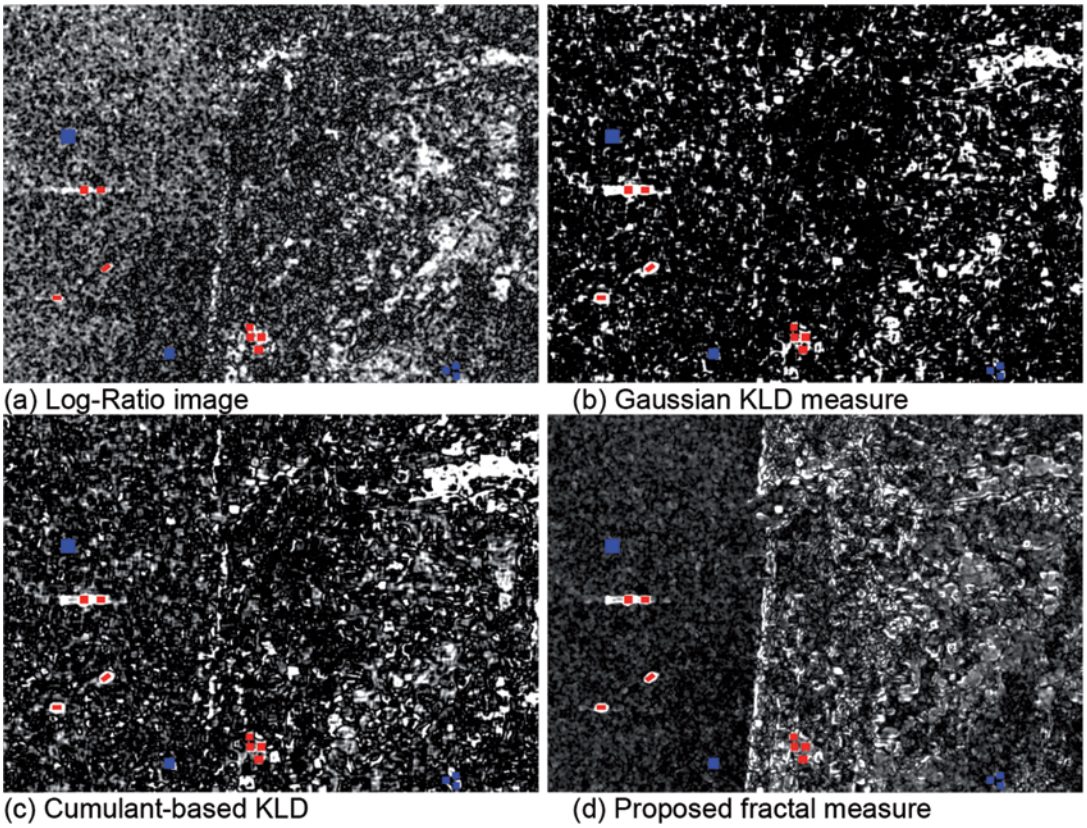

Fig. 4: Comparison of change measures. Red and blue pixels are reference regions for changed and unchange regions, respectively.

map of the Gaussian KLD are shown in Figs. 4(b) and 5(b), whereas the change measure and change map of the cumulant-based KLD are displayed in Figs. 4(c) and 5(c), respectively. The drawback of the Gaussian and cumulant-based KLD is that the SAR intensity statistics are not distributed normally and that employing an improper model might result in poor detection performance. The proposed fractal measure yields better performance in distinguishing changed and unchanged areas as compared to the Gaussian and cumulant-based KLD measures. It should be noted that the Gaussian and cumulant-based KLD and

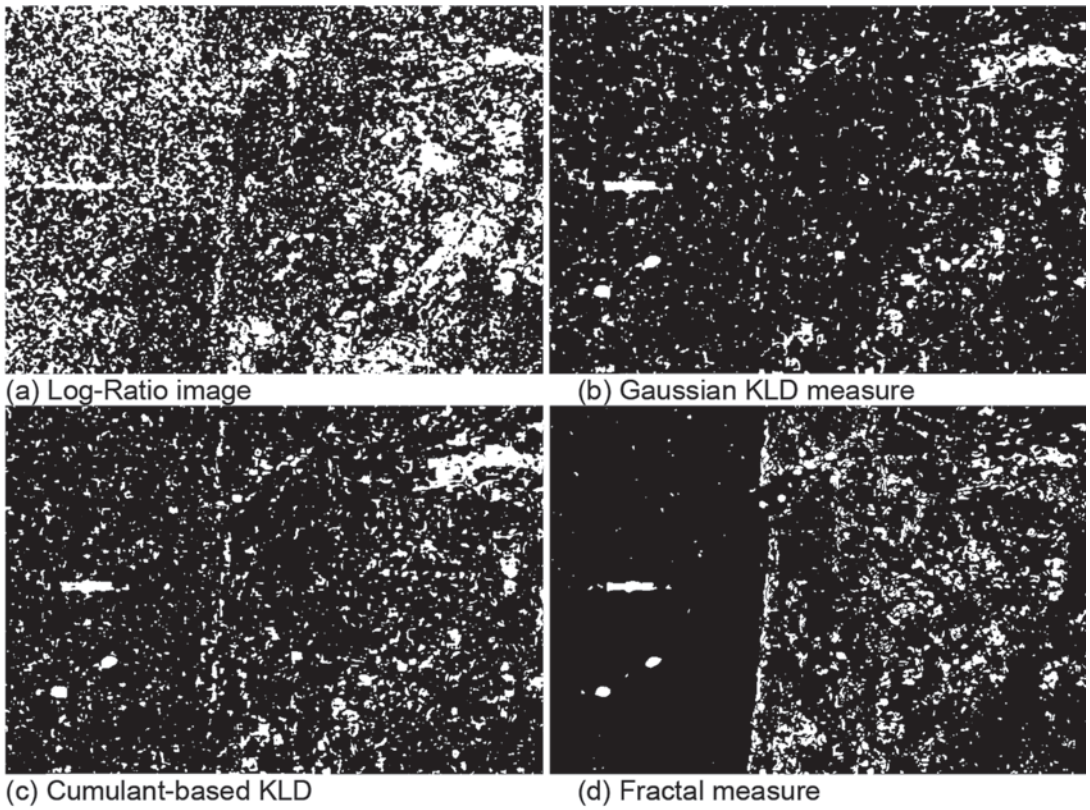

Fig. 5: Comparison of change maps obtained from different change measures for the change and unchange regions, respectively (KLD = Kullback-Leibler Divergence).

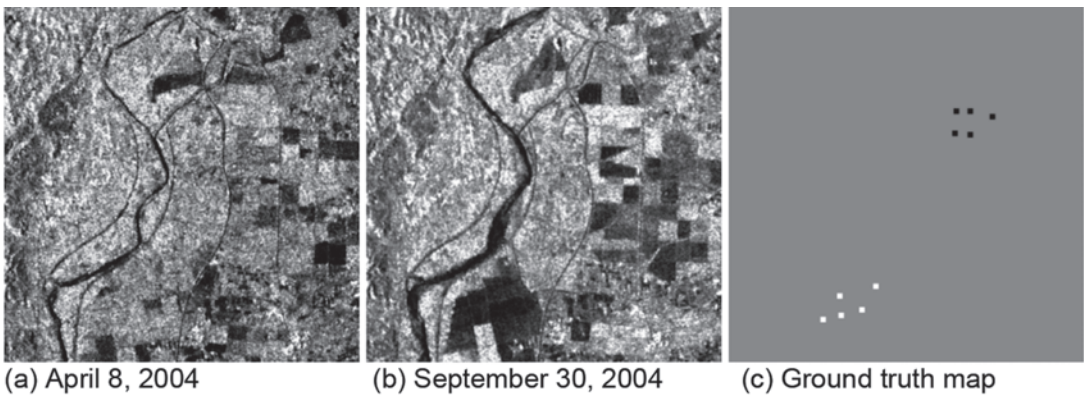

Fig. 6: Original ASAR alternative polarization mode (HV) images related to the second study area (Tuku).

also the proposed fractal measure are computed using the same window size (7×7). The high quality of the proposed fractal measure reveals that it can trace the changes regardless of the distribution model of the change intensity and gives satisfactory results in the presence of the speckle noise.

A quantitative comparison of the change detection algorithms is given Tab. 1, which is based on the reference regions in Fig. 4. The overall accuracy of the fractal measure (89.7 %) is better than the one achieved by the other implemented methods.

The second real dataset consists of a pair of ASAR images acquired in alternative polarization mode (HV) on-board ENVISAT in the area of Tuku (Taiwan). The original images were refined using enhanced Lee filter (Lopes et al. 1990) with a window size of 5 × 5 pixels. Fig. 6 displays the images of April 8, 2004 and September 30, 2004. The images have 30 m spatial resolution, and their size is 512 × 512 pixels. There are land cover changes due to both seasonal effects and agricultural practices. More than twenty survey sites located around a plantation field were identified

Tab. 2: Quantitative comparison of the change maps in the second real dataset (Tuku) (KLD = Kullback-Leibler Divergence).

	Unchanged		**Change**		
Overall Accuracy (%)	User's Accuracy (%)	Producer's Accuracy (%)	User's Accuracy (%)	Producer's Accuracy (%)	**Method**
92.8	96.9	94.2	76.7	86.3	**Log-Ratio**
97.0	96.9	99.5	97.5	85.3	**Gaussian KLD**
96.7	96.2	99.9	99.3	82.2	**Cumulant KLD**
97.6	97.3	99.9	99.3	87.5	**Fractal measure**

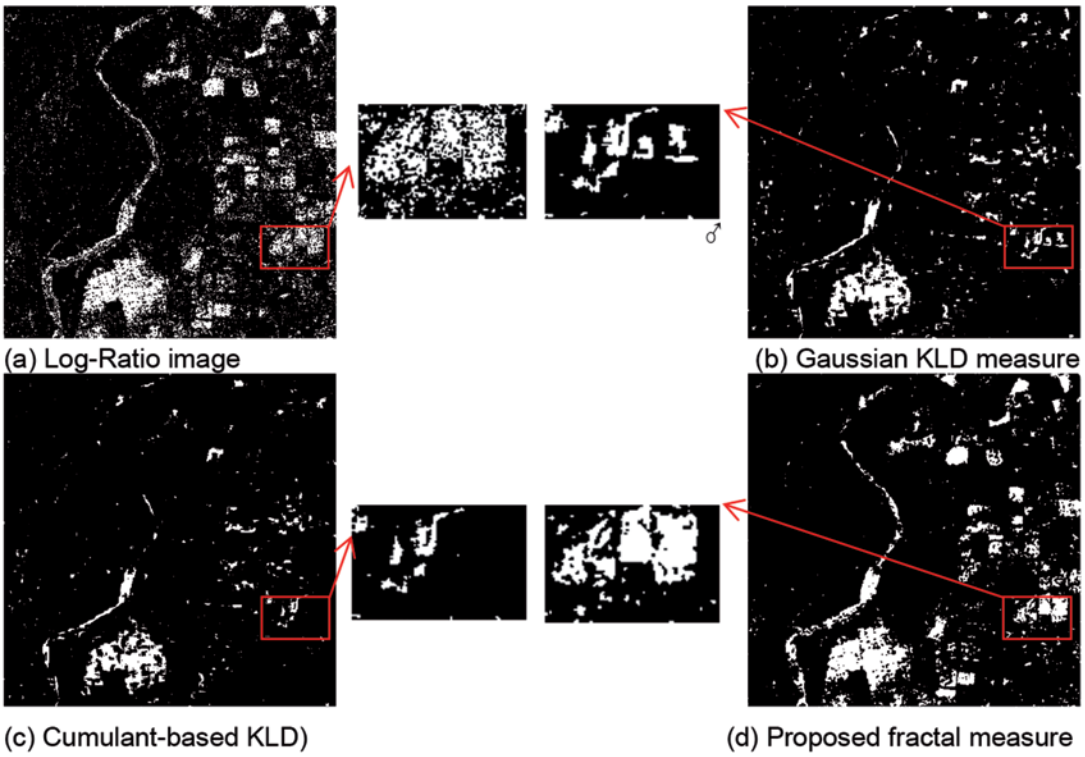

Fig. 7: Comparison of change maps obtained from different change measures.

for ground truth collections, aided by a land use map, an aerial photo, and SPOT images. In this test site, a total of seven land cover types were identified. They are: banana trees, grass, bare fields, rice fields, corn fields and rose fields. As these land cover types have changed frequently, the ground survey had to be conducted in accordance with the times the images were taken. There are 640 changed and unchanged pixels in the ground truth map (Fig. 6c), where white and black pixels correspond to the changed and unchanged areas, respectively. Each box contains 64 pixels.

Fig. 7 shows the change maps of the second test site using different change measures. As can be seen in Fig. 7 (a), the log-ratio gives many false detections. Comparing the results of Gaussian and cumulant-based KLD with the results of the fractal measure shows that the river and some landscape changes (in the right side of the image) were properly detected by the proposed measure because, unlike the statistical measure, the fractal measure can trace the changes regardless of a distribution model. A quantitative evaluation of the results is given in Tab. 2. The overall accuracy for the proposed method is 97.6 %. This value is slightly better than those achieved by the two KLD-based methods. The results of the evaluation based on the ground truth map shows the proposed measure's efficiency in comparison to the similarity measures and the classical log-ratio image.

4 Discussions and Conclusion

This paper proposed a new fractal measure for land use/cover change detection of SAR images. The proposed fractal measure is calculated by the combination of fractal and intensity information of original SAR images. Fractal dimension can be regarded as a statistical measure of the overall geometric complexity of image textures. So, the proposed fractal measure is sensitive to the texture changes. Applying a threshold to the proposed fractal measure, one can automatically take a binary decision at each pixel location to determine whether it is a change pixel or not. The threshold is computed from the distribution of the fractal measure using the well-known Otsu method. The proposed approach is compared to the classical log-ratio detector and other statistical similarity measures. Experiments have been carried out on both simulated and real data using different SAR images. Experimental results confirm the effectiveness of the proposed fractal measure. In particular, as expected, the proposed fractal measure is shown to be more suitable than the Gaussian and cumulant-based Kullback-Leibler detectors in distinguishing changed and unchanged areas. From the experimental results, it can be concluded that the main advantages of the proposed fractal measure are 1) that it uses both the fractal information and the intensity 2) that it is able to detect the change regardless of the distribution model of the change intensity, and 3) that it has high efficiency in change detection in various areas such as agriculture and water-bodies.

However, determining an optimal window size for fractal image computation is a question which still remains unanswered. Applying different window sizes may result in a different fractal dimension. It is more appropriate to use a smaller window in rough areas and a larger window for the smooth ones. Also, having the SAR images, the additional information like image coherence could be employed as a third index in the proposed measure. Such aspects will be studied as a future development of this work.

Acknowledgements

The authors would like to thank the venture business laboratory and the center for environmental remote sensing, Chiba University, Japan and National united university, Taiwan for the provision of the data. Also, we would like to extent our sincere appreciation to the reviewers and the editors for their great comments, which helped us to significantly improve the paper.

References

Astrium, 2012: http://www.astrium-geo.com/en/23-sample-imagery. – www.astrium-geo.com/en/23-sample-imagery (9.2.2013).

Bazi, Y., Bruzzone, L. & Melgani, F., 2005: An Unsupervised Approach Based on the Generalized Gaussian Model to Automatic Change Detection Multitemporal SAR Images. – IEEE Transaction on Geoscience and Remote Sensing **43** (4): 874–887.

Betti, A., Barni, M. & Mecocci, A., 1997: Using a wavelet-based fractal feature to improve texture discrimination on SAR images. – International conference on image processing **1:** 251–254.

Bovolo, F. & Bruzzone, L., 2008: An Adaptive Technique based on Similarity Measures for Change Detection in Very High Resolution SAR Images. – IEEE International Geoscience and Remote Sensing Symposium (IGARSS) **3:** 158–161.

Bujor, F., Trouvé, E., Valet, E., Niccolas, J. & Rudant, J., 2004: Application of log-cumulants to the detection of spatiotemporal discontinuities in multi-temporal SAR images. – IEEE Transaction in Geoscience and Remote Sensing **42** (10): 2073–2084.

Cola, L.D., 1989: Fractal analysis of classified Landsat scene. – Photogrammetric Engineering and remote sensing **55** (5): 601–610.

De Jong, S.M. & Burrough, P.A., 1995: A fractal approach to the classification of Mediterranean vegetation types in remotely sensed images. – Photogrammetric Engineering and Remote Sensing **61** (8): 1041–1053.

Erten, E., Reigber, A., Ferro-Famil, L. & Hellwich, O., 2012: A New Coherent Similarity Measure for Temporal Multichannel Scene Characterization. – IEEE Transactions on Geoscience and Remote Sensing **50** (7): 2185–2188.

Goodman, J., 1976: Some fundamental properties of speckle. – Journal of Optical Society of America **66** (11):145–1150.

Inglada, J. & Mercier, G., 2007: A new statistical similarity measure for change detection in multi-temporal SAR images and its extension to multi-scale change analysis. – IEEE Transactions of Geoscience and Remote Sensing **45** (5): 1432–1445.

Lopes, A., Touzi, R. & Nezry, E., 1990: Adaptive speckle filters and scene heterogeneity. – IEEE Transaction on Geoscience and Remote Sensing **28** (6): 992–1000.

Mallat, S.G., 1989: A theory for multi-resolution signal decomposition: the wavelet representation. – IEEE Transactions on Pattern Analysis and Machine Intelligence **11** (7): 674–693.

Mandelbrot, B.B., 1982: The Fractal Geometry of Nature. – W.H. Freeman and Company, New York.

Mercier, G., Moser, G. & Serpico. S.B., 2008: Conditional Copulas for Change Detection in Heterogeneous Remote Sensing Images. – IEEE Transactions of Geoscience and Remote Sensing **46** (5): 1428–1441.

Mcdonald, M.K., Varadan, V. & Leung, H., 2002: Chaotic behavior and non-linear prediction of airborne radar sea clutter data. – IEEE International conference of Radar: 331–337.

Myint, S.W., 2003: Fractal approaches in texture analysis and classification of remotely sensed data: Comparisons with spatial autocorrelation techniques and simple descriptive statistics. – International Journal of Remote Sensing **24** (9): 1925–1947.

Otsu, N., 1979: A Threshold Selection Method from Gray-Level Histograms. – IEEE Transactions on Systems, Man and Cybernetics **9** (1): 62–66.

Parra, C., Iftekharuddin, K. & Rendon, D., 2003: Wavelet Based Estimation of the Fractal Dimension in fBm Images. – IEEE International conference on neural engineering: 533–536.

Peitgen, H.O. & Saupe, D., 1987: The Science of Fractal Images. – Springer-Verlag, New York, USA.

Pentland, A.P., 1984: Fractal-based description of natural scenes. – IEEE Transaction on Pattern Analysis and Machine Intelligence 6 (6): 661–674.

Ramstien, G. & Raffy, M., 1989: Analysis of the structure of radiometric remotely-sensed images. – International Journal of remote sensing **10** (6): 1049–1073.

Shiyong, C., Mihai, D. & Gueguen, L., 2011: Information theoretical similarity measure for change detection. – Urban Remote Sensing Event (JURSE): 69–72.

Singh, A., 1989: Review Article: Digital Change Detection Techniques Using Remotely Sensed Data. – International Journal of Remote Sensing **10** (6): 989–1003.

Stewart, C.V., Moghaddam, B., Hintz, K.J. & Novak, L.M., 1993: Fractional Brownian motion models for Synthetic aperture radar imagery scene segmentation. – IEEE **81** (10): 1511–1522.

Sun, W., Xu, G., Gong, P. & Liang, S., 2006: Fractal analysis of remotely sensed images: A review of methods and applications. – International Journal of Remote sensing **27** (22): 4963–4990.

Sun, Y., Tian, J. & Liu, J., 2005: Two-band Infrared Data Fusion Method Based-on Fractal Dimension. – IEEE International Conference on Neural Networks and Brain **2:** 1197–1201.

Tzeng, Y.C, Chiu, S.H. & Chen, K.S., 2007: Change Detections from SAR Images for Damage Estimation Based on a Spatial Chaotic Model. – IEEE International Geoscience and Remote Sensing Symposium: 1926–1930, Barcelona, Spain.

Addresses of the Authors:

Hossein Aghababaee & Dr. Jalal Amini, Department of Surveying and Geomatic Engineering, University of Tehran, Iran, Tel.: +98-91-26443951, e-mail: {aghababaee}{jamini}@ut.ac.ir

Prof. Dr. Yu Chang Tzeng, Department of Electronic Engineering, National united university, Maio-Li, Taiwan, e-mail: john@nuu.edu.tw

Prof. Josaphat Tetuko Sri Sumantyo, Microwave Remote Sensing Laboratory, Center for Environmental Remote Sensing, Chiba University, Japan, e-mail: jtetukoss@faculty.chiba-u.jp

Manuskript eingereicht: Juni 2012
Angenommen: Januar 2013